Change of the Magnetic-Field Topology by an Ergodic Divertor and the Effect on the Plasma Structure and Transport

M. W. Jakubowski,[1,*] O. Schmitz,[1] S. S. Abdullaev,[1] S. Brezinsek,[1] K. H. Finken,[1] A. Krämer-Flecken,[1] M. Lehnen,[1] U. Samm,[1] K. H. Spatschek,[2] B. Unterberg,[1] R. C. Wolf,[1] and TEXTOR Team

[1]*Institut für Plasmaphysik, Forschungszentrum Jülich GmbH, EURATOM Association, Trilateral Euregio Cluster, D-52425 Jülich, Germany*

[2]*Institut für Theoretische Physik I, Heinrich-Heine-Universität, Düsseldorf, Germany*

(Received 8 June 2005; published 25 January 2006)

The magnetic-field perturbation produced by the dynamic ergodic divertor in TEXTOR changes the topology of the magnetic field in the plasma edge, creating an open chaotic system. The perturbation spectrum contains only a few dominant harmonics and therefore it can be described by an analytical model. The modeling is performed in the vacuum approximation without assuming a backreaction of the plasma and does not rely on any experimentally obtained parameters. It is shown that this vacuum approximation predicts in many details the experimentally observed plasma structure. Several experiments have been performed to prove that the plasma edge behavior is defined mostly by the magnetic topology of the perturbed volume. The change in the transport can be explained with the knowledge of only the magnetic structures; i.e., the ergodic pattern dominates the plasma properties.

DOI: 10.1103/PhysRevLett.96.035004 PACS numbers: 52.55.Fa, 52.55.Rk

Nonaxisymmetric static or dynamic helical magnetic perturbations are introduced in tokamak plasmas in order to investigate a broad spectrum of applications, such as the control of heat and particle transport by ergodic effects [1–4], island divertors [5], helical divertors [6], and the suppression of edge localized modes, so-called ELMs [7], by the stochastic fields [8]. The dynamic ergodic divertor (DED) [9] in the TEXTOR tokamak [10] has been installed to study a variety of questions connected to stochasticity in a plasma and the interaction of helical perturbations with magnetized plasmas [11]. Sixteen coils are aligned parallel to the field lines at the resonant flux surface ($q = 3$) resulting in a resonant coupling between plasma and perturbation magnetic fields. The base mode of the magnetic perturbation can be varied by the connections of the power supplies to the coils between $m/n = 12/4$, $6/2$, and $3/1$, where m, n refers to the poloidal and toroidal mode number. The "vacuum" calculations predict that the penetration depth of the perturbing field depends strongly on the base mode numbers. The $12/4$ mode affects the plasma only in the outermost layer (~6–7 cm), while the magnetic perturbation in the $3/1$ mode reaches the plasma core. The basic features of the DED are also discussed in [12,13].

The modeling of the magnetic-field topology is made with the ATLAS code [12], which is based on a model developed by Abdullaev *et al.* [14–16]. The model uses Hamiltonian formulation of the field line equations assuming linear superposition of the plasma equilibrium field and the magnetic perturbation of the DED coils in a vacuum approximation. The solutions of Hamilton equations for field lines are found using a fast running symplectic mapping [14]. In this Letter, it is shown that the plasma structures affected by the ergodic divertor is strongly correlated to the topology predicted by this "idealized" model. In addition to the studies by Evans *et al.* [4], here we have achieved a distinction between the effect of short and long connection lengths on plasma transport. Since the DED system produces a relatively simple perturbation field, it was possible to perform direct comparisons between the plasma structures and modeled magnetic-field topologies. The general properties of the plasma edge resulting from the DED were predicted in detail demonstrating that the changes in transport can be understood with the knowledge of the calculated field line structures.

Figure 1(a) shows a false-color image of the CIII light emission (i.e., coming from the electronic transition of C^{2+}), recorded by means of CCD camera equipped with an interference filter at $\lambda = 465$ nm, (discharge #95592: $I_{\text{plasma}} = 350$ [kA], $B_\varphi = 1.9$ [T], $a = 0.43$ [m], $R_a = 1.73$ [m], the base mode 12/4, $I_{\text{DED}} = 12$ [kA], $P_{\text{NBI}} = 0.8$ MW). The camera has a toroidal view, tangential to the inner wall (or divertor target plate), and observes the light pattern of CIII, which is located near to the surface, around the equatorial midplane. Each frame is recorded for 8 ms. The figure clearly shows the effect of the near field of the DED resulting in a deformation of the flux zones to the wall. Superimposed to the figure is a Poincaré plot visualizing the structure of the perturbed volume. For the Poincaré plot, magnetic-field lines are analyzed for up to 15 poloidal turns. One observes that the distribution of the CIII spectral line intensity not only follows the symmetry of the perturbation field, but it also strongly depends on the magnetic structures predicted by the model.

The perturbed volume is restricted to a few centimeters at the plasma edge ($r \gtrsim 40.5$ cm) and it surrounds the confined region of undestroyed flux surfaces (except for a few island chains, e.g., $m/n = 10/4$). At the boundary, the magnetic flux tubes have a relatively short connection length; this area forms the so-called laminar zone. The connection lengths of the field lines forming the laminar zone are

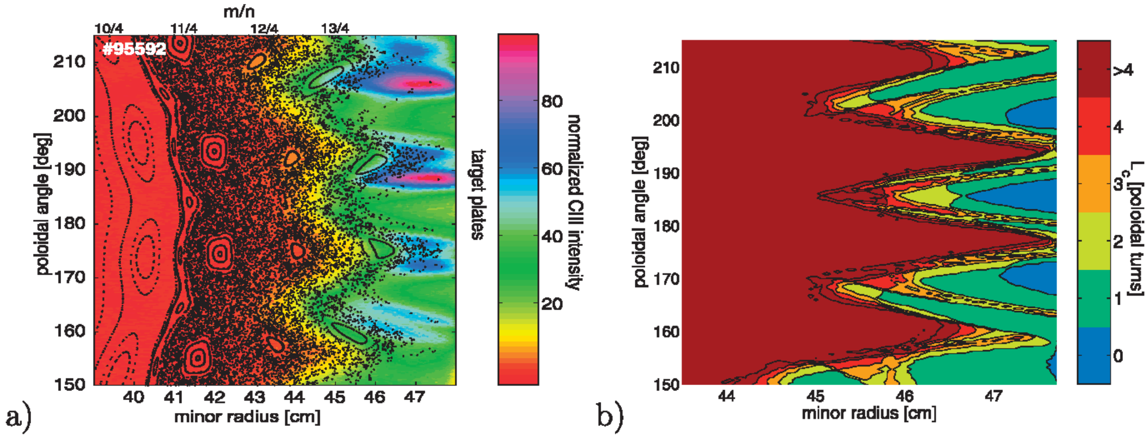

FIG. 1 (color). (a) The two-dimensional distribution of the CIII emission in the front of the DED coils for discharge #95592 overlayed with the Poincaré section visualizing the structure of the magnetic field calculated with the ATLAS code. The color bar indicates the intensity of the CIII line at 465 nm in the arbitrary units. The m/n numbers on the top of the figure indicate the island chains. (b) Corresponding laminar plot representing the contour plot of the field lines connection length calculated for the same conditions as in (a).

shorter then the Kolmogorov length, which is a measure of the e-folding length of the exponentially growing separation of neighboring trajectories [2]. The laminar zone is equivalent to the scrape-off layer of a poloidal divertor. However, the length of the flux tubes is not uniform but varies as shown in Fig. 1(b). It has been found previously that the flux tubes of similar connection lengths form continuous areas, and at the boundaries between the areas of different connection lengths, one finds fine scale structures of magnetic-field lines (named "fingers") which can, e.g., connect the ergodic zone with the wall [17,18]. The width and structure of the flux tubes and of the fingers is of particular interest for the plasma flow pattern toward the walls. The transport in the laminar zone is expected to be governed by the competition between the transport along the magnetic-field lines to the perpendicular one. The structure of the resulting heat flux pattern is discussed in [18].

In order to study the relevance of the laminar and ergodic zones for the plasma transport, measurements of the edge electron density and temperature were carried out by an active helium beam injection experiment located upstream of the divertor target plate, namely, at the equatorial plane at the low field side (LFS) [21]. The geometry of the beam is shown in the left graph in Fig. 2(a): the radial resolution of the beam is 1.2 mm and the divergence of the beam is marked with the black solid lines (~6° poloidally).

The radial structure of the electron temperature and density at different times of the discharge and the connection length are shown in Fig. 2(a). The electron temperature and density as a function of plasma minor radius during discharge #95895 ($I_{\mathrm{plasma}} = 350$ [kA], $B_\varphi = 1.9$ [T], $a = 0.46$ [m], $R_a = 1.73$ [m], the base mode 12/4, $I_{\mathrm{DED}} = 13$ [kA], $P_{\mathrm{NBI}} = 0.3$ MW) are presented as the red lines on the right-hand side of Fig. 2(a), whereas the blue and black curves show the electron density (top) and electron temperature (bottom) profiles measured before (blue curves) and after (black curves) the DED phase. The vertical green dash-dotted line at $r = 44$ cm visualizes the "last closed flux surface" (LCFS) in the limiter case. The drop in n_e and T_e is shifted inwards (toward smaller plasma radii) as compared to the non-DED case. For the non-DED case the region of the lowered electron pressure—scrape-off layer—is formed outside this LCFS. The reason becomes clear if one calculates the field line connection lengths for this region, which is presented as the green dashed line (right axis). The region of low connection lengths, $L_c \simeq 2$ poloidal turns, at plasma minor radius of $r \approx 0.42$ [m] represents the flux tube connecting the outer equatorial midplane with the divertor target plates [12]. This flux tube is surrounded by the field lines with longer connection lengths.

Complementary information is given in Fig. 2(b). Here the poloidal profiles of n_e and T_e are presented. During discharge #95924 ($I_{\mathrm{plasma}} = 400$ [kA], $B_\varphi = 1.9$ [T], $a = 0.46$ [m], $R_a = 1.73$ [m], the base mode 12/4, $I_{\mathrm{DED}} = 11$ [kA], $P_{\mathrm{NBI}} = 0.3$ MW) the perturbation field was swept with very low frequency (1 Hz) over the angle indicated by $\Delta\theta$ in order to visualize the poloidal structure of the laminar zone. The results for different plasma radii are indicated on the right-hand side of the Fig. 2(b). The coordinates of the measured profiles are shown on the left-hand side of Fig. 2(b) as the dashed lines overlaid with the corresponding laminar plot. The structures in the laminar plot are averaged in order to "simulate" the spatial resolution of the thermal helium beam. The drop in both n_e and T_e is well correlated with the $L_c = 1$ poloidal turn flux tube. One has to note that the minimum of the electron density $r = 42$ cm, whereas the minimum of T_e falls between $r = 42.5$ cm and $r = 43$ cm. This indicates that there is a difference between heat and particle transport in the laminar region. It has been found in related measurements that flux tubes formed in the laminar zone

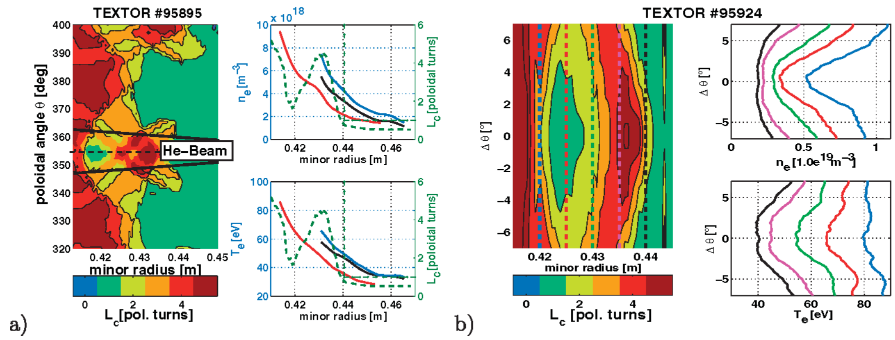

FIG. 2 (color). The influence of the laminar zone on the plasma electron temperature and density. (a) The radial profiles of the electron density (top right) and electron temperature (bottom right). The red curves present the data measured during the DED phase, the blue curves the data before the DED phase, and the black one the data after the DED phase. Green lines (right ordinate): calculated with the ATLAS-code connection lengths of the field lines for the coordinates of the measured profiles: DED case (dashed line); non-DED case (dash-dotted line). On the left, the laminar plot visualizing the magnetic-field topology during discharge #95895 is presented beam. Black lines visualize the geometry of the thermal helium beam. (b) On the right, the poloidal variation of the plasma electron density (top) and temperature (bottom) measured during the slow (1 Hz) sweep of the perturbation field. On the left, the effective laminar plot visualizing the magnetic topology. The data represent a convolution of calculated L_c values and the spatial resolution of the diagnostic. Dashed lines indicate the coordinates at which n_e and T_e profiles are measured.

intersect the divertor target plates and thus create the sinks for the particle and heat flux. It results in the drop of the temperature and density in the laminar zone as seen in the n_e and T_e profiles. One can distinguish two sources of particles—the plasma core and the divertor wall—and only the core is the source for the energy. The particle and heat fluxes, which are reaching the flux tube at $r \approx 0.42$ m and $\theta \approx 355°$ in Fig. 2(a), stream toward the target plates and miss the red isolated area of Fig. 2(a) with the longer connection lengths at $r \approx 0.43$ m and $\theta \approx 355°$. The local maximum in the plasma density profile is probably due to "cold" particles recycling from the plasma wall. The effects of the applied perturbation field are observed immediately and we do not observe any threshold or delay for the onset of the ergodization as it has been reported for the onset of tearing modes [11].

The best confirmation of the resonant nature of the ergodic divertor concept is the strong variation of the edge plasma properties with the edge safety factor q_a. For these investigations, a series of discharges has been performed in which the plasma current was ramped down or up. In addition, the value of B_φ was slightly varied from discharge to discharge in order to obtain more points in the T_e profile, which is measured by the electron cyclotron emission diagnostic (ECE). In Fig. 3 the change of the electron temperature measured by ECE is presented. The color scale represents the relative change of the electron temperature. The graph is overlayed with the contour plot of the field line connection lengths calculated for the same parameters. One notices that the electron temperature depends strongly on the structure of the magnetic-field lines.

To understand these results, one has to consider the properties of the transport in the perturbed volume. As the particles follow the magnetic-field lines, they can move across the ergodic layer. This results in the enhancement of the effective cross-field diffusion coefficients. The diffusion of the particles streaming along the magnetic-field lines is normally written as $D_{\mathrm{fl}} c_s$, where D_{fl} is the field line diffusion coefficient and c_s is the sound speed. In the case of open chaotic systems the quasilinear approximation (see, e.g., [2]) fails and is replaced by numerically determined local field line diffusion coefficients [14], which are of the order of 2–4 $\times 10^{-6}$ m^2/m. Thus, the effective heat transport coefficients is about 4 times larger than the anomalous heat diffusion coefficients given in [19]—$\chi_{\mathrm{erg}}/\chi_\perp = 3.5$–4.4 in the highly ergodized case.

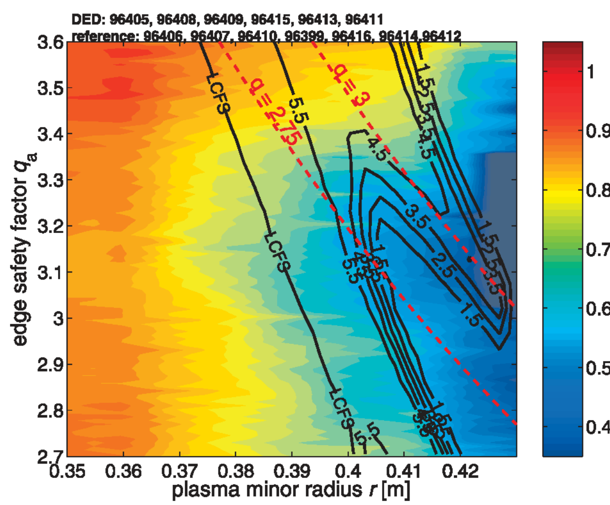

FIG. 3 (color). The contour plot of the drop in the electron temperature in the plasma edge measured by the ECE [20] as a function of the plasma minor radius (abscissa) and the value of the safety factor at the plasma edge—q_a (ordinate). The profiles obtained for the DED case were divided by the profiles measured for analogous discharge without the DED. The solid black lines represent the contour plot of the calculated connection lengths. The red dashed lines indicates the position of the $q = 3$ and $q = 2.75$ surfaces.

The transport in the laminar regime is mostly parallel to the field lines, where one finds the flux tubes, which channel the flow of heat and particles to the targets. Transport is a result of a balance between the parallel and the cross-field transport but with the complication of the 3D structure of the boundary. The plasma flow pattern in the laminar zone is highly complicated because the ergodic divertor forms flux tubes with different connection length and different stagnation points in close proximity. As the strength of the magnetic perturbation in the 12/4 mode is relatively weak, one expects that the significant change of the plasma parameters would happen in the case of dominating laminar zone.

At high values of the edge safety factor the ergodization is rather weak. Therefore the electron temperature is modified in a moderate way only in the volume of very short connection lengths with $L_c \approx 1$ poloidal turn. This effect is most pronounced at low and medium plasma densities. At $q_a < 3.4$, the position of the individual resonances reach their optimal position and the influence of the DED grows strongly. In the range of connection lengths of 4.5 poloidal turns $< L_c < \infty$ (where the $L_c = \infty$ is inside the line marked as the LCFS), an ergodic region is found and the electron temperature drops by 30%. In the laminar zone T_e is already 2 times smaller in the DED case as compared to the non-DED case. The largest influence of the DED on the electron temperature profile happens when the new area with the short connection lengths is opened up ($q_a \approx 3.2$, $r = 0.41$ m). At this condition, the perturbed volume is dominated by the laminar zone. The heat and particles are directed toward the divertor plates, which results in enhanced T_e drop. With the decrease of q_a, the topology of the ergodic and laminar domains change. A comparison of the structure of the connection lengths to the position of the $q = 3$ and $q = 2.75$ flux surfaces shows that the flux surfaces is not a simple function of the distances of the individual resonances to the perturbing coils. The structure of the magnetic-field lines becomes more complicated due to the pitch of the field lines changing from the high field side to the LFS. However, it turns out that the position of the resonant surfaces plays the main role. One can see that the maximum of ergodization falls into the conditions where the laminar zone is formed by the flux surfaces with safety factor close to 3. When these surfaces ''leave'' the plasma, the ergodization weakens, which is immediately followed by a reduction of the electron temperature drop.

In conclusion, a thorough analysis of the plasma properties in the presence of an ergodized edge has been performed. The evolution of plasma parameters in the perturbed volume can be explained with the knowledge of the magnetic-field topology. The plasma structures and transport are closely related to the structure of the field lines as calculated with the ATLAS code. It has been shown that the resonant ergodic pattern dominates the plasma properties at the plasma edge. The field lines with short connection length (i.e., laminar zone) influence mostly the plasma edge transport and structures. For the cases discussed here (12/4 mode), the vacuum approximation is valid; i.e., it was not necessary to take into account the backreaction of the plasma onto the applied perturbation. However, in case of a deeper penetration of the perturbation field with a higher amplitude (obtained with the base mode $m/n = 3/1$) the tearing modes were triggered on the $q = 2$ and 3 magnetic surfaces [11], showing the limitations of the vacuum approximation.

This work was partially supported by the Sonderforschungsbereich 591 of the Deutsche Forschungsgemeinschaft.

*Electronic address: ma.jakubowski@fz-juelich.de

[1] A. Lichtenberg and M. Liberman, *Regular and Stochastic Motion* (Springer-Verlag, Berlin, 1983).

[2] P. Ghendrih, A. Grosman, and H. Capes, Plasma Phys. Controlled Fusion **38**, 1653 (1996).

[3] B. Unterberg *et al.*, in Proceedings of the 20th IAEA Fusion Energy Conference, Portugal, 2004, available on CD-ROM only (File No. EX/P5-33).

[4] T. E. Evans, R. A. Moyer, and P. Monat, Phys. Plasmas **9**, 4957 (2002).

[5] R. König *et al.*, Plasma Phys. Controlled Fusion **44**, 2365 (2002).

[6] N. Ohyabu *et al.*, Nucl. Fusion **34**, 387 (1994).

[7] T. E. Evans *et al.*, Phys. Rev. Lett. **92**, 235001 (2004).

[8] T. E. Evans, R. K. W. Roeder, J. A. Carter, and B. I. Rapoport, Contrib. Plasma Phys. **44**, 235 (2004).

[9] Special issue on DED, edited by K. H. Finken [Fusion Eng. Des. **37**, 335 (1997)].

[10] O. Neubauer *et al.*, Fusion Sci. Technol. **47**, 76 (2005).

[11] R. C. Wolf *et al.*, Nucl. Fusion **45**, 1700 (2005).

[12] M. W. Jakubowski, S. S. Abdullaev, K. H. Finken, and TEXTOR Team, Nucl. Fusion **44**, S1 (2004).

[13] K. H. Finken *et al.*, Phys. Rev. Lett. **94**, 015003 (2005).

[14] S. Abdullaev, K. Finken, and K. Spatschek, Phys. Plasmas **6**, 153 (1999).

[15] S. S. Abdullaev, K. Finken, M. Jakubowski, S. Kasilov, and M. Kobayashi, Nucl. Fusion **43**, 299 (2003).

[16] S. S. Abdullaev, Nucl. Fusion **44**, S12 (2004).

[17] K. H. Finken, S. S. Abdullaev, A. Kaleck, and G. H. Wolf, Nucl. Fusion **39**, 637 (1999).

[18] M. W. Jakubowski, S. S. Abdullaev, K. H. Finken, M. Lehnen, and TEXTOR Team, J. Nucl. Mater. **337–339**, 176 (2005).

[19] M. Kobayashi, Y. Feng, F. Sardei, D. Reiter, K. H. Finken, and D. Reiser, Nucl. Fusion **44**, S64 (2004).

[20] G. Waidmann, P. C. de Vries, A. Kramer-Flecken, H. P. Eulenberg, and K. Huxhagen, Rev. Sci. Instrum. **68**, 492 (1997).

[21] O.Schmitz, Ph.D. thesis, Heinrich-Heine-Universität, 2006.